

# Saw-tooth softening/stiffening model

J.G. Rots

*Faculty of Architecture, Delft University of Technology, Delft, The Netherlands.*

S. Invernizzi

*Faculty of Architecture, Delft University of Technology, Delft, The Netherlands.*

*Department of Structural Engineering & Geotechnics, Politecnico di Torino, Torino, Italy.*

**ABSTRACT:** A sequentially linear saw-tooth continuum model which captures the nonlinear response via a series of linear steps is presented. In the model, the softening stress-strain curve with negative slope is replaced by a saw-tooth diagram of positive slopes, while the incremental-iterative procedure is replaced by a scaled sequentially linear procedure. Mesh-size objectivity is achieved by adjusting both the peaks and the ultimate strain of the saw-tooth diagram to the size of the finite elements, keeping the fracture energy invariant. First, considering large-scale dog-bone specimens in direct tension, it will be demonstrated that the model is capable of automatically providing the snap-back response. Furthermore, the bifurcation problem is circumvented as the scaling process triggers the lowest non-symmetric equilibrium path. Secondly, the model is extended from an isotropic to an orthotropic format, taking into account the direction of cracking and the anisotropy of the induced damage. In this way, the model can compare with classical fixed smeared crack models. This improvement allows for studying reinforced concrete structures, in which compressive struts develop parallel to the crack directions. Finally, the effectiveness of the enhanced model is proven considering a long-embedding tension-pull specimen and a slender reinforced beam, showing a good ability to capture both the load-displacement curve and the crack pattern.

**Keywords:** saw-tooth sequentially linear, snap-back, snap-through, reinforced concrete

## 1 INTRODUCTION

Negative stiffness due to softening is a major problem in computational modeling of concrete fracture. It may lead to numerical instability and divergence of the incremental-iterative procedure. This holds especially for the analysis of medium- and large-scale structures. Cracks in structures are accompanied by dips, ripples, jumps and snap-backs in the load-displacement response. This behavior is typical of un-reinforced structures (e.g. facades) where the amount of elastic energy stored in the structure is large compared to the fracture energy consumed in crack or crush propagation, but also of reinforced structures (e.g. tension-pull specimens or RC beams) where each primary crack gives a release or drop followed by a new ascending portion in the load-displacement curve. To try and solve such problems, users have to resort to arc-length or indirect control schemes, which are cumbersome and often inadequate when the peaks are irregular or the snap-backs sharp.

As an alternative, this paper presents a sequentially linear saw-tooth continuum model, which captures the nonlinear response via a series of linear steps. The softening stress-strain curve with negative slope is replaced by a saw-tooth diagram of positive slopes, while the incremental-iterative procedure is replaced by a scaled sequentially linear procedure (Rots, 2001). After a linear analysis, the critical element, i.e. the element for which the stress is closest to the current peak in the saw-tooth diagram, is traced. Next, the stiffness of that element is reduced and the process is repeated. The sequence of critical states governs the global load-displacement response, while the elements with reduced stiffness reveal the softened areas. The advantage is that there is no such thing as ‘negative incremental stiffness’, as the secant linear (saw-tooth) stiffness is always positive. The analysis always ‘converges’. Mesh-size objectivity is achieved by adjusting both the peaks and the ultimate strain of the saw-tooth diagram to the size

of the finite elements, keeping the fracture energy invariant (Rots & Invernizzi, 2003).

The paper starts with a summary of the description of the model. Next, the procedure to achieve mesh-size objectivity is reviewed both with respect to the mesh size and the number of saw-teeth, considering a notched beam in bending.

Subsequently, the case of large-scale dog-bone specimens in direct tension is considered. It will be demonstrated that the sequentially linear model is capable of automatically providing the snap-back response. Bifurcations in these symmetric fracture specimens are circumvented in a natural manner as the scaling procedure always picks the ‘lowest’ equilibrium solution associated with the ‘most critical’ element, even for numerical round-off in a symmetric case.

Finally, the model is improved to take into account the intrinsic anisotropy due to crack nucleation and softening. This is a crucial aspect in order to describe reinforced structures, in which the reinforcement (*ties*) is balanced against compressive *struts* that develop parallel to the crack directions.

Two different reinforced structures are considered, namely the reinforced tension-pull specimen, and a slender reinforced concrete beam.

In both cases, the response shows local peaks and snap-backs associated with the subsequent development of primary cracks starting from the rebar. Comparisons between incremental-iterative solutions and sequentially linear solutions are given and the behavior is interpreted in terms of crack spacing and crack width.

## 2 ISOTROPIC SAW-TOOTH SOFTENING

### 2.1 *Global sequentially linear procedure*

The basic idea is to look for the equilibrium configuration via secant approximations with restarts from the origin. The softening diagram is approximated by a saw-tooth curve and linear analyses are carried out sequentially (Rots 2001). This is similar to procedures for fracture analysis on lattices (Schlangen & van Mier 1992, Beranek & Hobbelman 1995), where little beam elements are removed rather than continuum elements reduced.

The global procedure is as follows. The structure is discretized using standard elastic continuum elements with assigned tensile strength.

Subsequently, the following steps are carried out:

- Add the external load as a unit load.
- Perform a linear elastic analysis.
- Extract the critical element from the results. The critical element is the element for which the principal tensile stress is closest to its current strength. This principal tensile stress criterion is widely accepted in mode-I fracture mechanics of quasi-brittle materials.
- Calculate the critical global load as the unit load times the current strength divided by stress of the critical element.
- Extract also a corresponding global displacement measure, so that later an overall load-displacement curve can be constructed.
- Reduce the stiffness and strength, i.e. Young’s modulus  $E$  and tensile strength  $f_t$  of the critical element, according to a saw-tooth tensile softening stress strain curve as described in the following.
- Repeat the previous steps for the new configuration, i.e. re-run a linear analysis for the structure in which  $E$  and  $f_t$  of the previous critical element are reduced.
- ..... Repeat again, etc. ....

### 2.2 *Saw-tooth softening model via stepwise reduction of Young’s modulus*

The way in which the stiffness and strength of the critical elements are progressively reduced constitutes the essence of the model. A very rough method would be to reduce  $E$  to zero immediately after the first, initial strength is reached. This elastic perfectly brittle approach, however, is likely to be mesh dependent as it will not yield the correct energy consumption upon mesh refinement (Bažant & Cedolin, 1979). In this study, the consecutive strength and stiffness reduction is based upon the concept of tensile strain softening, which is fairly accepted in the field of fracture mechanics of concrete (Bažant & Oh, 1983).

The tensile softening stress-strain curve is defined by Young’s modulus  $E$ , the tensile strength  $f_t$ , the shape of the diagram, e.g. a linear or exponential diagram, and the area under the diagram. The area under the diagram represents the fracture energy  $G_f$  divided by the crack band width  $h$ , which is a discretisation parameter associated with the size, orientation and integration scheme of the finite element. Although there is some size-dependence, the fracture energy can be considered to be a material property. This softening model usually governs nonlinear constitutive behavior in an incremental-iterative strategy. Please note that

here we adopt the curve only as a 'mother' or envelope curve that determines the consecutive strength reduction in sequentially linear analysis. In the present study, attention is confined to a linear softening diagram, but extension to any other shape of the diagram is possible. For a linear softening diagram, the ultimate strain  $\varepsilon_u$  of the diagram reads:

$$\varepsilon_u = \frac{2G_f}{f_t h}, \quad (1)$$

In a sequentially linear strategy, the softening diagram can be imitated by consecutively reducing Young's modulus as well as the strength. Young's modulus can e.g. be reduced according to:

$$E_i = \frac{E_{i-1}}{a}, \quad \text{for } i = 1 \text{ to } N \quad (2)$$

with  $i$  denoting the current stage in the saw-tooth diagram,  $i-1$  denoting the previous stage in the saw-tooth diagram and  $a$  being a constant. When  $a$  is taken as 2, Young's modulus of a critical element is reduced by a factor 2 compared to the previous state.  $N$  denotes the amount of reductions that is applied in total for an element. When an element has been critical  $N$  times, it is removed completely in the next step.

The reduced strength  $f_{ii}$  corresponding to the reduced Young's modulus  $E_i$  is taken in accordance with the envelope softening stress-strain curve:

$$f_{ii} = \varepsilon_u E_i \frac{D}{E_i + D}, \quad (3)$$

with

$$E_i = \frac{E}{a^i}, \quad (4)$$

and

$$D = \frac{f_t}{\varepsilon_u - \frac{f_t}{E}}, \quad (5)$$

being the tangent to the tensile stress-strain softening curve. Note that this is the softening curve in terms of stress versus *total* strain, i.e. the sum of elastic strain and crack strain of an imagined cracked continuum.

The model always provides a solution: the secant saw-tooth stiffness is always positive, so that ill-conditioning or divergence does not appear in sequentially linear analysis. An advantage of the model is that the regular notions of fracture

mechanics, like the principal tensile stress criterion, the envelope strength and fracture energy are maintained which helps in reaching realistic energy consumption and toughness as observed in experiments.

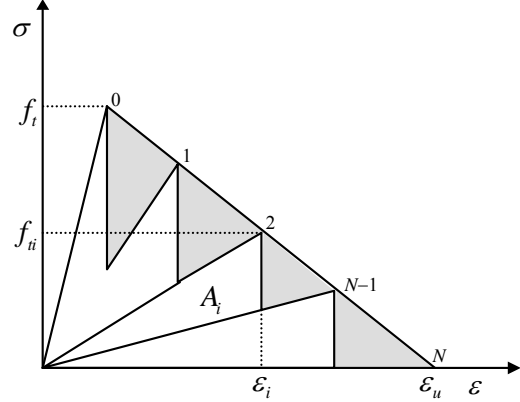


Figure 1. Saw-tooth softening approximation scheme, the underestimated area is shown in gray.

### 2.3 Mesh regularization

The concept of smeared crack basically assumes that the localized crack is distributed over a continuum finite element, provided that the crack opening  $\delta$  is equal to the element strain  $\varepsilon$  times the so called crack band width  $h$  (for lower-order elements often equal to the element size). In order to achieve mesh-size objectivity, the ultimate strain  $\varepsilon_u$  in smeared crack models is usually adjusted to  $h$  according to Eq. (1) for linear softening, Bazant & Oh (1993). In previous works (Rots & Invernizzi, 2003), it appeared that such adjustment is not sufficient to guarantee mesh-size objectivity for the case of the sequentially linear model. In fact, due to the saw-tooth approximation of the softening curve, the dissipated energy is always less than the theoretical one, i.e. the one referring to the smooth 'mother' softening curve. Moreover, the underestimation of the dissipated energy depends not only on the number of teeth, but also on the mesh size, since the ultimate strain depends on the crack band width. When finer meshes are considered, i.e. for a small value of  $h$ , the slope of the linear softening branch decreases and the area underestimation becomes more important.

In order to provide a correct regularization procedure and achieve mesh independence, it is first of all necessary to provide a useful expression for the actual area beneath the saw-tooth curve.

Referring to the scheme in Fig. 1, the formula is the following:

$$A = \sum_{i=0}^{N-1} A_i = \sum_{i=0}^{N-1} \frac{1}{2} \varepsilon_i f_u b_i, \quad (6)$$

where the index  $i$  refers to the triangular decomposition of the whole area.

The parameter  $b_i$  varies depending on the saw-tooth approximation method. In the case of stepwise Young's modulus reduction, it is the following:

$$b_i = \begin{cases} \left(1 - \frac{1}{a}\right) & 0 \leq i < N-1 \\ 1 & i = N-1 \end{cases}. \quad (7)$$

The basic idea, thus, is to update the tensile strength, or the ultimate strain, or even both, in order to keep the dissipated energy invariant. In other words, the area  $A^*$ , under the updated constitutive law, becomes invariant and equal to:

$$A^* = \frac{G_f}{h}. \quad (8)$$

Eq. 8 shows clearly that not only the number of teeth, but also the mesh size (i.e. the crack band width  $h$ ) comes into play.

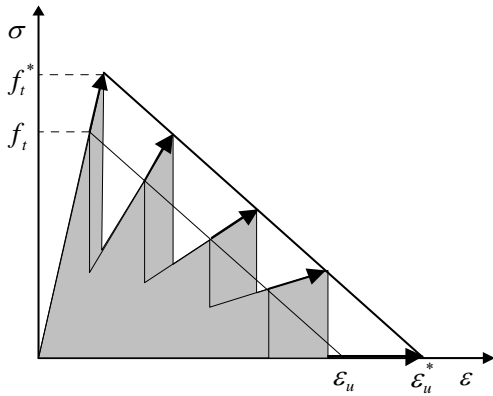


Figure 2. Regularization scheme with both the ultimate strain and the tensile strength update, keeping constant the softening modulus  $D$ .

Although in principle different approaches can be followed, it has been proved that the most effective technique is to update both the tensile strength and the ultimate strain. Therefore, the updated strength  $f_t^*$  and the ultimate strain  $\varepsilon_u^*$  will be determined as follow:

$$\begin{cases} f_t^* = k \cdot f_t \\ \varepsilon_u^* = k \cdot \varepsilon_u \end{cases}, \quad (10)$$

where  $k$  can be determined numerically in such a way that the new area satisfies Eq. 9 (see Fig. 2). After some analytical manipulation of Eq. 8, a closed form expression for the parameter  $k$  can be obtained:

$$k = \sqrt{\frac{\frac{G_f}{h}}{\sum_{i=0}^{N-1} \frac{1}{2} \frac{f_u^2}{E_i} b_i}}. \quad (12)$$

#### 2.4 Notched beam

A symmetric notched beam of total length 500 mm, span 450 mm, height 100mm, thickness 50 mm and notch depth 10 mm was selected for analysis. The distance between the loading points in the symmetric four-point loading scheme is 150 mm. Five different meshes were used (Fig. 3). These meshes have a symmetric center crack band of 20 mm, 10 mm, 5 mm, 2.5 mm and 1.25 mm width respectively. Four-node linear elements were used.

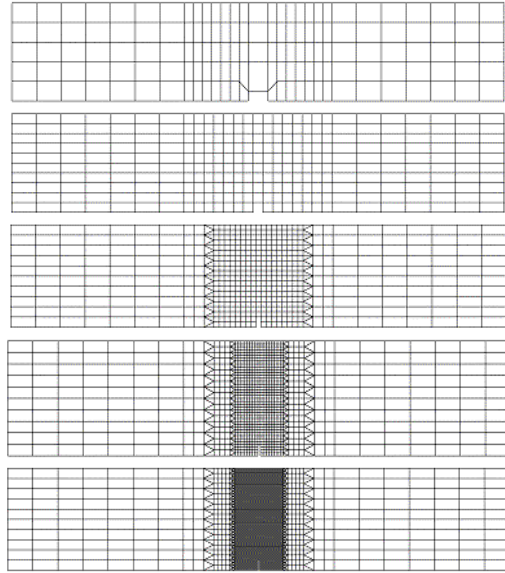


Figure 3. Meshes considered in the analysis, respectively referred in the following as very coarse, coarse, medium, fine and very fine.

Load displacement curves are shown in Fig. 4, for each mesh when a ten teeth approximation is adopted. It is evident that the sequentially linear results are in good agreement with the nonlinear analysis regardless the mesh size. When a larger number of teeth is chosen, the resemblance becomes even better. A detailed analysis can be found in Rots & Invernizzi (2003).

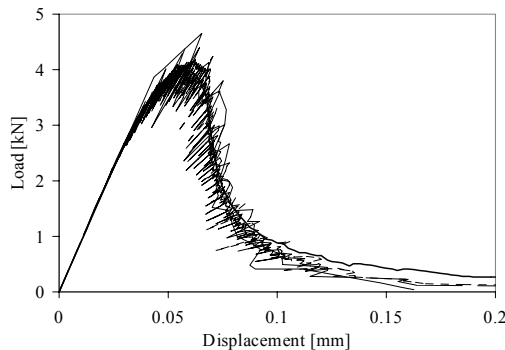


Figure 4. Load displacement diagrams, five different meshes, ten teeth. All the curves are coherent and closely resemble the reference peak load (continuous line).

### 3 LARGE-SCALE DOG-BONE SPECIMENS IN DIRECT TENSION

The case study concern direct tensile tests carried out on large-scale dog-bone concrete specimens (van Vliet, 2000). In order to prove the ability of the saw tooth model to capture the structural snap-back, we considered the largest size among the entire series, denominated as *type F* ( $D=1600$  mm;  $r=1160$  mm). Experimental load-displacement curves, shown in Figure 5, were obtained under indirect displacement control, adopting a gauge length that was sufficiently short. The mechanical parameters obtained by the test were adopted for the numerical analysis, i.e. a nominal tensile strength  $f_t=2.31$  N/mm<sup>2</sup> and a fracture energy  $G_f=0.1411$  N/mm. A linear softening tail was assumed.

#### 3.1 Smearred crack nonlinear analysis

Prior to the sequentially linear analysis, a standard nonlinear analysis was performed. Linear isoparametric plane stress elements were used to discretize both the plain concrete and the steel platens. The two element rows at top and bottom of Figure 6a represent the steel platens.

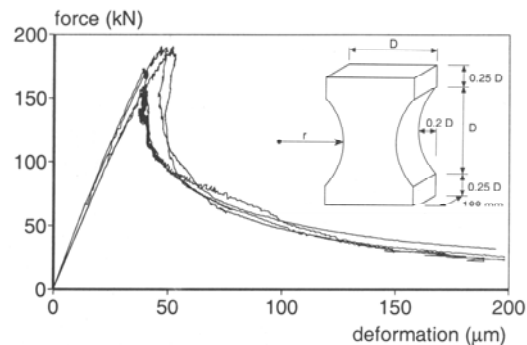


Figure 5. Scheme of the dog-bone specimen and experimental load-displacement curves (van Vliet, 2000).

The boundary condition was carefully taken into account modeling the central hinges at top and bottom used to de-constrain the structure. The influence of the boundary condition on post peak behavior is crucial (van Vliet, 2000), both from an experimental and numerical point of view. The outcome of the numerical simulation depends on the control parameter. If the simulation is performed under load control, only the pre-peak branch of the load displacement curve can be traced. If the simulation is carried out with displacement control, on the other hand, the load displacement curve can be traced a bit further, till the snap-back phenomenon take place. After that the analysis can be continued, but there is a sudden jump on the lower equilibrium path (i.e. snap-back). The third possibility is to adopt an indirect load control, e.g. with the arc-length methods (Crisfield 1984, de Borst 1987). In this case, it is finally possible to obtain the whole load displacement curve.

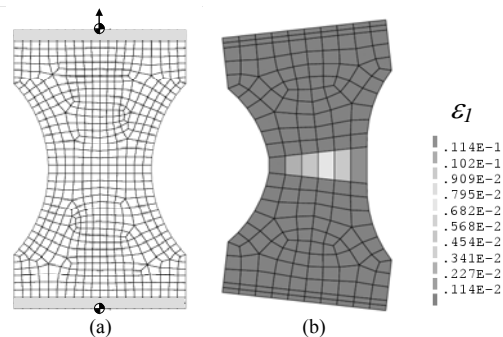


Figure 6. Mesh of the dog bone specimen (a); deformed mesh and principal tensile strain contour referring to the last sequentially linear step (b).

Unfortunately, although in principle it is possible to get the solution, the choice of load steps or of

the arc-length options and indirect control parameters, is usually cumbersome, and difficulties increases with increasing the size (i.e. the brittleness) of the structure.

Another problem with the nonlinear analysis is the bifurcation. In fact, as soon as the peak load is reached, due to the symmetry of the structure, two different equilibrium paths arise. The symmetric path is unstable, and is not encountered experimentally, while the non-symmetric stable path is characterized by crack propagation from one side only of the dog-bone specimen. Consequently, a negative pivot arises, in the LDU scheme, due to the bifurcation of equilibrium, and it is necessary to introduce a perturbation of symmetry (geometrical or material) in the model, in order to get a solution.

### 3.2 Isotropic sequentially linear analysis

The same mesh and the same mechanical parameters were adopted for the saw tooth analysis (Figure 6a). The analysis was carried out with a ten teeth approximation. The load displacement curve is depicted in Figure 7, and shows a very good agreement with the smeared crack nonlinear analysis. It is worth noting that both curves compare well with experimental results. The advantage of the sequentially linear analysis is that the system is always positive definite, so that a solution is always found at each step. The sequence of linear solutions automatically provides the snap-back.

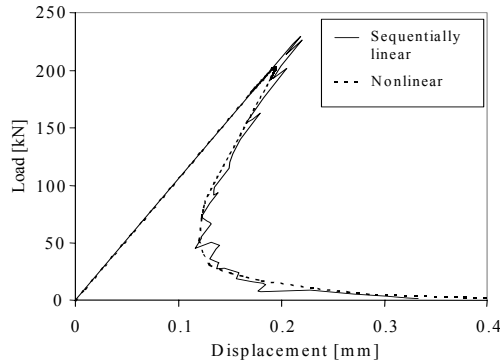


Figure 7. Snap-back in the load displacement curve.

When the solution is considered to be too coarse, showing an irregular spiky pattern, it is sufficient to refine the discretization, i.e. decreasing the mesh, or to increase the number of teeth.

Another advantage is that the scaling process mentioned in Section 2.1 involves that the numerical round-off implicitly breaks the symmetry of the model. There is no need to add imperfections to the model in order to follow the stable equilibrium path. At the same time, the indirect control of the structure is not required any more, since the effective control parameter is the propagating damage itself.

The sequentially linear simulation provides not only the correct load displacement curve, but also the correct damage localization in the central part of the sample, induced by the dog-bone shape of the specimen, as shown in Fig. 6b.

## 4 ANISOTROPIC SEQUENTIALLY LINEAR: FIXED CRACKING

Although the isotropy assumption taken above allows for the simulation of cracking of plane concrete in direct tension or bending (i.e. when the phenomenon is basically driven by a localized crack in a one-dimensional stress field), a substantial improvement is necessary when dealing with reinforced concrete. In fact the isotropic reduction of stiffness is a rather rough approximation, and does not represent the compressive struts that develop parallel to the cracks.

Therefore, in analogy to the pioneering approach of Rashid (1968), the initial isotropic stress-strain law can be replaced by an orthotropic law upon crack formation, with the axes of orthotropy being determined according to a condition of crack initiation. As far as the present work concerns, the crack plane is kept constant after the crack is nucleated. Moreover, only one crack per element is considered.

Referring to the plane stress situation, and to a local coordinate system oriented parallel to the crack plane, the following constitutive relation is assumed:

$$\begin{Bmatrix} \sigma_{nn} \\ \sigma_{tt} \\ \sigma_{nt} \end{Bmatrix} = \begin{bmatrix} \frac{E_i}{1-\nu^2} & \frac{\nu E_i}{E} & 0 \\ \frac{\nu E_i}{E} & \frac{E}{1-\nu^2} & 0 \\ 0 & 0 & \beta G \end{bmatrix} \begin{Bmatrix} \varepsilon_{nn} \\ \varepsilon_{tt} \\ \varepsilon_{nt} \end{Bmatrix}, \quad (14)$$

where  $n$  is the normal to the crack,  $t$  the crack plane,  $E_i$  the reduced Young modulus according to

the sequentially linear scheme, and  $\beta$  the so-called shear retention factor. The equation can be rewritten in compact form as follow:

$$\boldsymbol{\sigma}_{nt} = \mathbf{D}_{nt} \boldsymbol{\varepsilon}_{nt} \quad (15)$$

In addition to Young's modulus, also the shear retention factor and the Poisson ratio decrease with increasing crack opening. In the present implementation a stepwise reduction is assumed:

$$\begin{cases} \beta_i = \frac{N-i}{N} \\ \nu_i = \frac{N-i}{N} \end{cases}, \quad 0 \leq i \leq N, \quad (16)$$

where  $i$  is the current tooth, and  $N$  the number of teeth adopted in the discretization. Given the following transformations for the strain and stress vectors:

$$\begin{cases} \boldsymbol{\varepsilon}_{nt} = \mathbf{T}_\varepsilon(\phi) \boldsymbol{\varepsilon}_{xy} \\ \boldsymbol{\sigma}_{nt} = \mathbf{T}_\sigma(\phi) \boldsymbol{\sigma}_{xy} \end{cases}, \quad (17)$$

eq. 14 can be easily transposed in terms of global stress and strain components by pre- and post-multiplication with the transformation matrices:

$$\boldsymbol{\sigma}_{xy} = \mathbf{T}_\sigma^{-1}(\phi) \mathbf{D}_{ns} \mathbf{T}_\varepsilon(\phi) \boldsymbol{\varepsilon}_{xy}. \quad (18)$$

The above improved constitutive law was implemented in the general sequentially linear scheme.

#### 4.1 Reinforced tension-pull specimen

A long-embedment tension-pull specimen is considered (Gijbsers & Hehemann, 1977). The steel is modeled by truss elements, and the concrete by axis-symmetry elements.

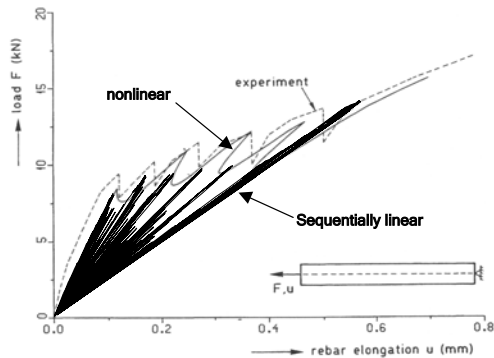


Figure 8. Load-displacement curves: experimental (Gijbsers & Hehemann, 1977), nonlinear (Rots, 1985) and sequentially linear analysis.

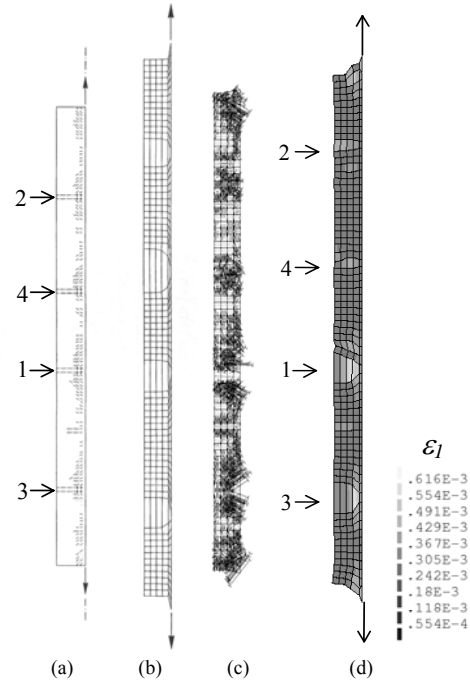


Figure 9. Long-embedment tension-pull specimen. Nonlinear cracking (a), nonlinear deformed mesh (b). Sequentially linear compressive struts (c) and deformation (d).

Perfect bond between steel and concrete was assumed. The strength of the concrete was assigned via a random generation of tensile strength (mean  $f_t=3.0$  N/mm<sup>2</sup>, standard deviation equal to 0.5 N/mm<sup>2</sup>).

In Fig. 8, results from nonlinear smeared analysis and experiments are compared with the load-displacement curve for the anisotropic sequentially linear model. Although the behavior is more brittle, the sequentially linear analysis is in good agreement with the nonlinear results, being able to describe snap-back and snap-through behavior. In Fig. 9, the comparison is made in terms of crack localization and resulting deformed meshes. Four primary cracks emerge. In particular, Fig. 9c shows how compressive struts arise in the anisotropic saw-tooth analysis. With the former isotropic version of the model, the struts (compressive cones) could not develop and an incorrect crack evolution was obtained.

#### 4.2 Reinforced concrete beam

In this example we investigate the performance of the anisotropic saw tooth model with respect to a practical engineering problem, namely a reinforced

beam which fails in bending and which was tested by Walraven (1978). The finite element idealization for the beam is shown in Fig. 10. Eight-noded plane-stress elements were used to represent the concrete and three-noded truss element for the reinforcement. Perfect bond was assumed between the concrete and reinforcement.

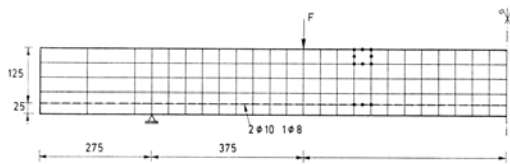


Figure 10. Finite element idealization of the RC beam.

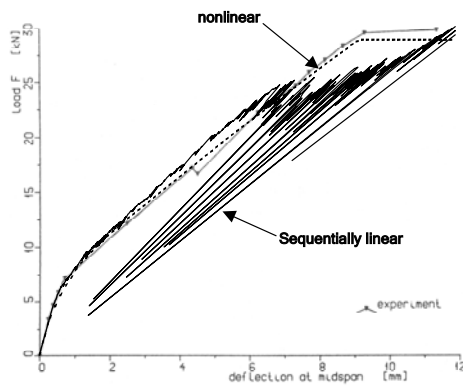


Figure 11. Load-displacement curves: Experimental (Walraven, 1978), nonlinear (Rots, 1985) and sequentially linear analysis.

Both a nonlinear smeared crack and anisotropic sequentially linear analysis were performed. The results are shown in Fig. 11, where a good agreement between the sequentially linear and nonlinear or experimental data is found. The sequentially linear analysis cannot yet take into account the yielding of the reinforcement; on the other hand it is numerically stable and able to emphasize the brittle behavior of the final part of the load displacement curve.

## 5 CONCLUSIONS

The saw-tooth sequentially linear model has been reviewed in order to emphasize its ability to capture snap-back and snap-through instabilities automatically, without numerical problems. The model has thus been improved taking into account the damage anisotropy induced by cracking. The effectiveness of the model to capture basic features

of reinforced structures has been evaluated by two examples: the long-embedment tension-pull test, and a slender RC beam in bending.

## 6 ACKNOWLEDGEMENTS

Financial support from Delft Cluster, COB and the Netherlands Technology Foundation STW is acknowledged. The research was carried out using an adapted version of DIANA.

## 7 REFERENCES

- Bažant, Z.P. & Cedolin, L. 1979. Blunt crack band propagation in finite element analysis. *ASCE J. Engineering Mechanics Division* 105(2): 297-315.
- Bažant, Z.P. & Oh, B.H. 1983. Crack band theory for fracture of concrete. *Materials and Structures* 16(93): 155-177.
- de Borst, R. 1987. Computation of post-bifurcation and post-failure behavior of strain-softening solids. *Computers & Structures* 25(2): 211-224.
- Rots, J.G. 1985. Bond-slip simulations using smeared cracks and/or interface elements. *Res. Report 85-01, Struct. Mech.*, Dept. of Civil Engng., Delft Univ. of Techn.
- Rots, J.G. 2001. Sequentially linear continuum model for concrete fracture. In de Borst R., Mazars J., Pijaudier-Cabot G., van Mier J.G.M. (eds), *Fracture Mechanics of Concrete Structures*: 831-839. Lisse: Balkema
- Rots, J.G. & Invernizzi S. 2003. Regularized saw-tooth softening, In Bičanić N., de Borst R., Mang H., Meschke G. (eds), *Computational Modelling of Concrete Structures*: 599-617. Lisse: Balkema.
- Schlangen, E. & van Mier J.G.M. 1992. Experimental and numerical analysis of micro-mechanisms of fracture of cement-based composites. *Cement & Concrete Composites* 14: 105-118.
- Beranek, W.J. & Hobbelman, G.J. 1995. 2D and 3D-Modelling of concrete as an assemblage of spheres: reevaluation of the failure criterion. In Wittmann F.H. (ed.), *Fracture mechanics of concrete structures. Proc. FRAMCOS-2*: 965-978. Freiburg: Aedificatio.
- Crisfield, M.A. 1984. Difficulties with current numerical models for reinforced-concrete and some tentative solutions. F. Damjanic, N. Bicanic et al. (eds), *Proc. Int. Conf. Computer Aided Analysis and Design of Concrete Structures*. Part I: 331-358.
- Gijsbers, F.B.J. & Hehemann, A.A. 1977. Some tensile tests on reinforced concrete, *Report BI-77-61*, TNO Inst. For Building Mat. And Struct., Delft.
- Rashid, Y.R. 1968. Analysis of prestressed concrete pressure vessels, *Nuclear Engng. And Design* 7(4): 334-344.
- Walraven, J.C. 1978 The influence of depth on the shear strength of lightweight concrete beams without shear reinforcement. *Report 5-78-4* Stevin Laboratory, Delft University of Technology, Delft.